Scaffolds for Sustained Release of Ambroxol Hydrochloride, a Pharmacological Chaperone that Increases the Activity of Misfolded β-Glucocerebrosidase

Hamidreza Enshaei, Brenda G. Molina, Luis J. del Valle, Francesc Estrany, Carme Arnan, Jordi Puiggalí, Núria Saperas and Carlos Alemán**

H. Enshaei, B. G. Molina, Dr. L. J. del Valle, Dr. F. Estrany, Prof. Dr. J. Puiggalí, Dr. N. Saperas, Prof. Dr. C. Alemán
Departament d'Enginyeria Química and Barcelona Research Center for Multiscale Science and Engineering, EEBE, Universitat Politècnica de Catalunya, C/ Eduard Maristany, 10-14, Ed. I2, 08019 Barcelona, Spain
E-mail: nuria.saperas@upc.edu and carlos.aleman@upc.edu

Dr. C. Arnan
Centre for Genomic Regulation (CRG), The Barcelona Institute of Science and Technology, 08003 Barcelona, Catalonia, Spain
Universitat Pompeu Fabra (UPF), 08002 Barcelona, Catalonia, Spain

Prof. Dr. J. Puiggalí, Prof. Dr. C. Alemán
Institute for Bioengineering of Catalonia (IBEC), The Barcelona Institute of Science and Technology, Baldiri Reixac 10-12, 08028 Barcelona, Spain

Keywords: Electrospinning; Gaucher's disease; Misfolding diseases; Lysosomal storage disorders; Poly(ε-caprolactone); Polyester; Release regulation

Abstract

Ambroxol is a pharmacological chaperone (PC) for Gaucher disease that increases lysosomal activity of misfolded β-glucocerebrosidase (GCase) while displaying a safe toxicological profile. In this work we have developed different poly(ε-caprolactone) (PCL)-based systems to regulate the sustained release of small polar drugs in physiological environments. For this purpose, ambroxol has been selected as test case since the encapsulation and release of PCs using polymeric scaffolds have not been explored yet. More specifically, ambroxol has been successfully loaded in electrospun PCL microfibers, which have been subsequently coated with additional PCL layers using dip-coating or spin-coating. The time needed to achieve 80% release of loaded ambroxol increases from ~15 min for uncoated fibrous scaffolds to 3 days and 1 week for dip-coated and spin-coated systems, respectively. Furthermore, we have proved that the released drug maintains its bioactivity, protecting GCase against induced thermal denaturation.

1. Introduction

Existing polymer-based drug delivery systems can be divided into two groups based on their mode of administration. The first relies on systemic delivery and consists of nano-materials such as polymer nanoparticles, liposomes, and dendrimers. These delivery vehicles, which are predominantly intended for oral or intravenous administration, find their target by passive diffusion or by triggering the release of payload from an environment-responsive nano-carrier using a local stimulus (*i.e.* pH, temperature, etc). However, systemic delivery may result in suboptimal drug therapeutic concentration, leading to erroneous conclusions regarding agent efficacy. The second group of polymer delivery vehicles (and focus of this research) includes controlled release drug delivery depot systems for implantation inside or adjacent to the target tissue. The majority of these local polymer device systems are biodegradable so as to circumvent a second surgery for device removal and to avoid a chronic foreign-body immune response. The polymers used in these systems are often hydrophobic in nature, and are ideally suited for long-term delivery and internal stabilization of sensitive water-insoluble hydrophobic drugs. Nevertheless, long-term delivery of polar drugs remains a challenge since they are rapidly extracted from the vehicle by the aqueous environment of the target, making difficult the achievement of sustained concentrations in detriment of the localized therapy.

On the other hand, pharmacological chaperone (PC) therapy is an emerging therapeutic approach for the treatment of protein misfolding diseases, which consists of a diverse group of disorders associated with the incorrect folding of specific proteins.[1] Some misfolding diseases are due to missense protein mutations that cause abnormal conformations and the consequent loss of the function. PC therapy is based on the use of small molecule ligands (*i.e.* the PCs) that selectively bind and stabilize mutated

proteins, thus, favoring their correct conformation.[2] Therefore, the activity of the mutated proteins is partially rescued, which has a favorable impact on the patient status and the rate of disease progression.

This work aims to design a long-term delivery polymer vehicle for polar hydrophilic drugs, which does not affect the bioactivity. For this purpose, we have chosen ambroxol hydrochloride (AH; Scheme 1), a mucolytic agent that potentiates the activity of sodium channels, which has been shown to act also as a PC for the lysosomal enzyme β-glucocerebrosidase (GCase). Mutations in the GCase gene cause Gaucher's disease, which is the most prevalent lysosomal storage disease. AH has been shown to promote and stabilize the proper folding of GCase in the endoplasmic reticulum.[3] The PC role played by AH in the enhancement of the activity of misfolded GCase has been demonstrated using *in vitro*[3,4] and *in vivo* models.[5] Furthermore, recent clinical trials in patients with Gaucher disease showed that AH led to substantial clinical improvement.[6]

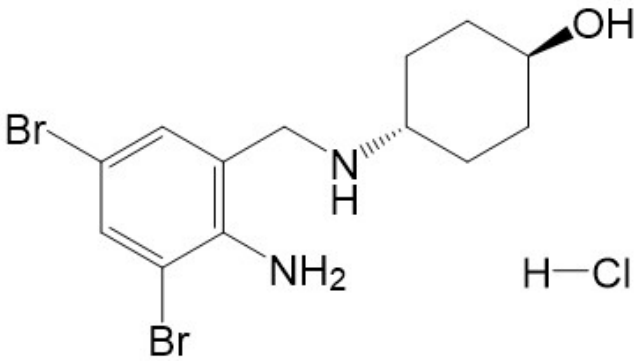

Scheme 1. Chemical structure of AH.

Although AH can be administered orally or through intravenous injection, the tissue distribution is unfortunately rather heterogeneous (*e.g.* AH is much easily distributed in lung tissue than in brain tissue)[3] and, therefore, its encapsulation into carriers to regulate its release might be highly desirable from a therapeutic point of view. In

general, on demand local delivery of drug molecules provides a means for effective drug distribution and dosing, fulfilling requirements for a variety of therapeutic applications while reducing the adverse effects of systemic drug administration.[7,8] Indeed, recent advances have facilitated the use of various cues, such as UV- and visible-wavelength light, NIR radiation, magnetic field, ultrasound or electrical stimulation to trigger the release of different types of drugs from smart materials.[8-10] Besides, as the utilization of PCs is a therapeutic paradigm recently launched, the encapsulation and release of these small ligands using polymeric scaffolds have not been explored yet. Studies oriented towards this aim might be useful in a near future.

In this work we have engineered poly(ε-caprolactone) (PCL) layered systems consisting of electrospun microfibers (MFs), which successfully encapsulate the PC, protected with a coating that regulates the release. This protection has been achieved by sandwiching the loaded MFs between two outer spin-coated nanomembranes (NMs) or by dip-coating the loaded MFs into a polymer solution. Electrospinning is a well-known electrostatic technique that uses a high voltage field to charge the surface of a polymer solution droplet at the end of a capillary tube and induce the ejection of a liquid jet towards a grounded target (collector).[11] Morphology of fibers obtained in the collector depends on the solution properties (*e.g.* viscosity, dielectric constant, volatility and concentration) and operational parameters (*e.g.* strength of the applied electric field, deposition distance and flow rate), which should be conveniently addressed.[12] In recent years, electrospinning experienced a fast developing to simultaneous treatment of multiple fluids for creating complex nanostructures, such as core-shell, tri-layer from the coaxial and tri-axial electrospinning processes.[13] Although these core-shell nanostructures can provide tunable drug sustained release profiles,[14] the after-treatment of nanofibers from a single-fluid blending process represents another way for achieving

an improved sustained release. We have focused on this second approach which, due to its macro-scale nature, has the advantage of being more easily scaled-up.

On the other hand, PCL has attracted an increasing interest in recent decades due to its biodegradability, easy processability and suitability for tissue engineering applications.[15] The use of this aliphatic polyester for biomedical applications was approved by the USA Food and Drug Administration (FDA) in the seventies and PCL can be found in many common sutures and suture components. Although small hydrophobic drugs were successfully loaded and smartly released from PCL electrospun fibers,[10,16] the polarity of the studied PC has motivated the design of the PCL-based layered systems to obtain slow and sustained release of active AH in physiological media. Thus, the polar hydrogen bonding acceptor and donor groups identified in the chemical structure of AH (Scheme 1) are expected to favor a very fast release rate in hydrophilic physiological environments, making difficult its dosage when continued administration is required. In order to avoid such limitation, which is can be extrapolated to other polar and hydrophilic drugs, in this work we propose different coating strategies to regulate the release depending on the necessities.

2. Methods

2.1. Materials

PCL (Aldrich, UK, Mn:80,000), AH (Sigma, Italy), chloroform (Scharlau, Spain; stabilized with amylene, 99.8% pure), acetone (Sigma, South Korea, 99.9% pure) formic acid (FA; Panreac, E.U., 98% pure), and 2,2,2-trifluoroethanol (TFE; Sigma, USA, 99% pure) were used as received.

2.2. Electrospinning

PCL is frequently electrospun from chloroform or chloroform:acetone solutions[15b,16] but AH is insoluble in such organic solvents. However, AH can be solubilized in chloroform:acetone if either TFE or FA is present. Accordingly, electrospun MFs were prepared by dissolving PCL in a 2:1 *v/v* chloroform:acetone mixture while AH was dissolved in either TFE or FA. Electrospun AH-loaded PCL MFs coming from TFE and FA solutions have been denoted PCL/AH(TFE) and PCL/AH(FA), respectively, while unloaded PCL MFs (controls) are labelled as PCL(TFE) and PCL(FA). Although PCL and AH concentrations, as well as the electrospinning operational conditions, were optimized to avoid the formation of undesirable beads and droplets in PCL/AH(TFE) and PCL/AH(FA) MFs, only the optimized parameters are described below.

Specifically, PCL/AH(TFE) MFs were prepared by dissolving 1.3 g of PCL in 7.5 mL of a 2:1 *v/v* chloroform:acetone mixture using an incubator (37 ºC and 120 rpm) for 12 h, while 0.0375 g of AH were added to 2.88 mL of TFE and vortexed extensively until completely dissolved. Then both solutions were thoroughly mixed together by additional strong vortexing. On the other hand, electrospun PCL/AH(FA) MFs were obtained by dissolving 1.3 g of PCL in 9.85 mL of the same 2:1 *v/v* chloroform:acetone solution. In this case, the PC was prepared by adding 0.0375 g of AH to 50 μL of 2:1 v/v chloroform:acetone. Then, 0.1 mL of FA was immediately added and the mixture was intensively vortexed until the drug was completely dissolved. Again, both solutions were mixed together with vigorous and extensive shaking. PCL(TFE) and PCL(FA) controls were prepared using identical procedures and solvents but without including the AH. The concentration of drug in PCL/AH(TFE) and PCL/AH(FA) MFs was below the cytotoxic threshold.[3]

Electrospinning was carried out in a non-conductor chamber. Solutions were loaded in a 10 mL BD Discardit (Becton Dickson Co., Franklin Lakes, NJ, USA) plastic syringe for delivery through a blunt-tipped (*i.e.* without bevel) 18 G needle (inner diameter 0.84 mm). The flow rate and the needle tip-collector distance were 5 mL/h and 15 cm, respectively, for PCL/AH(TFE) and PCL(TFE), whereas these parameters changed to 4 mL/h and 25 cm, respectively, for PCL/AH(FA) and PCL(FA). The voltage, which was applied through a high-voltage Gamma High Voltage Research (ES30-5W) power supply, was 20 kV in all cases. All electrospinning experiments were carried out at room temperature.

2.3. Spin-coating and dip-coating

Poly(ε-caprolactone) nanomembranes (PCL NMs) were spin-coated for the preparation of multilayered AH-loaded systems. Spin-coating was performed with a spin-coater (WS-400BZ-6NPP/A1/AR1 Laurell Technologies Corporation). In all cases, the first PCL NM was spin-coated using a Teflon® square plate as substrate (area: 2×2 cm^2), which was previously cleaned by sonication in three different solvents (5 min each): milli-Q water, acetone and ethanol. For the fabrication of the PCL NMs, 1 mL of a 60 mg/mL polymer solution in acetone was first spin-coated onto the Teflon® substrate at 750 rpm for 1 min (first layer). After placing a 1×1 cm^2 piece of an AH-loaded fibrous mat on top of this layer, a second PCL NM was created by spin-coating under the same conditions (top layer). Alternatively, coating was also performed by dipping the fibrous mat for 3 seconds in a 60 mg/mL PCL solution in acetone (dip-coating). In all cases, multilayered systems with non-drug-containing fibrous mats were also prepared as controls.

2.4. Characterization of electrospun MFs and NMs

The morphology and texture of electrospun MFs was examined by scanning electron microscopy (SEM) using a Focus Ion Beam Zeiss Neon 40 instrument (Carl Zeiss, Germany). Fibrous mats, which were cut in 1×1 cm^2 samples, were mounted on a double-sided adhesive carbon disc and sputter-coated with a thin layer of carbon to prevent sample charging problems. All samples were observed at an accelerating voltage of 5 kV. Diameters of electrospun MFs were measured with the SmartTiff software from Carl Zeiss SMT Ltd.

Atomic force microscopy (AFM) studies were conducted to obtain topographic and phase images of the surface of MFs using TAP 150-G silicon tapping probes. Images were obtained with an AFM Dimension microscope using the NanoScope IV controller under ambient conditions in tapping mode. The root mean square roughness (R_q), which is the average height deviation taken from the mean data plane, was determined using the statistical application of the NanoScope Analysis software (1.20, Veeco).

FTIR spectra were recorded with a Fourier Transform FTIR 4100 Jasco spectrometer (Jasco Analytical Instruments, Easton, USA) in the 4000–600 cm^{-1} range. An attenuated total reflection (ATR) system with a heated Diamond ATR Top-Plate (model MKII Golden Gate™, Specac Ltd., Orpington, UK) was used.

Raman spectra were obtained using a Renishaw inVia Qontor confocal Raman microscope. The Raman setup consisted of a laser (at 532 nm with a nominal 250 mW output power) directed through a microscope (specially adapted Leica DM2700 M microscope) to the sample, after which scattered light is collected and directed to a spectrometer with a 2400 lines·mm^{-1} grating. The exposure time was 10 s, the laser power was adjusted to 0.1% of its nominal output power depending on the sample, and each spectrum was collected with five accumulations.

UV-vis absorption spectra were recorded to confirm the presence of AH in electrospun MFs. For this purpose, fibrous mats were cut into 1×1 cm^2 samples, weighted and dissolved in 200 μL of chloroform. Then, 1 mL of milli-Q water was added and vortexed for 5 min to extract the PC. The two phases were separated by centrifuging at 12900 rpm for 3 min. Spectra of the aqueous phase were obtained using a UV-vis-NIR Shimadzu 3600 spectrophotometer equipped with a tungsten halogen visible source, a deuterium arc UV source, a photomultiplier tube UV-vis detector, and a InGaAs photodiode and cooled PbS photocell NIR detectors. Spectra were recorded in the absorbance mode at room temperature, the wavelength range and bandwidth being 190-400 nm and 2 nm, respectively.

X-Ray photoelectron spectroscopy (XPS) analyses were performed in a SPECS system equipped with a high-intensity twin-anode X-ray source XR50 of Mg/Al (1253 eV / 1487 eV) operating at 150 W, placed perpendicular to the analyzer axis, and using a Phoibos 150 MCD-9 XP detector. The X-ray spot size was 650 μm. The pass energy was set to 25 and 0.1 eV for the survey and the narrow scans, respectively. Charge compensation was achieved with a combination of electron and argon ion flood guns. The energy and emission current of the electrons were 4 eV and 0.35 mA, respectively. For the argon gun, the energy and the emission current were 0 eV and 0.1 mA, respectively. The spectra were recorded with a pass energy of 25 eV in 0.1 eV steps at a pressure below 6×10^{-9} mbar. These standard conditions of charge compensation resulted in a negative but perfectly uniform static charge. The C 1s peak was used as an internal reference with a binding energy of 284.8 eV. The surface composition was determined using the manufacturer's sensitivity factors.

Contact angle (CA) measurements were conducted using the sessile drop method. 0.5 μL of milliQ water drops were deposited onto the surface of the electrospun mats,

which were cut into rectangular pieces and fixed on a holder, and recorded after stabilization with the equipment OCA 15EC (DataPhysics Instruments GmbH, Filderstadt). The SCA20 software was used to measure the CA, which is shown here as the average of at least 40 measures for each condition.

2.5. AH-Release experiments

AH-loaded and unloaded (controls) fibrous mats were cut into small squares (1×1 cm^2), which were weighed and placed into Eppendorf tubes. Phosphate buffered saline (PBS) solution of pH 7.4 was considered as the release medium. Assays, which were performed in triplicate, were carried out by immersing sample mats in 1 mL of the release medium and using a rotating agitator. The medium was removed at predetermined time intervals and replaced by fresh one. The removed medium was used to quantify the released AH by measuring its absorbance in a UV-vis-NIR Shimadzu 3600 spectrophotometer as described above. Finally, the mats were dissolved in chloroform and the residual PC was extracted for quantification. The calibration curve (y= 6.838·x, R^2= 0.999) was obtained by plotting the absorbance against AH concentration from triplicate samples (Figure S1). On the other hand, PCL controls evidenced that the polymer degradation products do not interfere with the AH concentration measurements in long term assays.

2.6. Evaluation of the activity of released AH

Cell lysates, containing the lysosomal enzyme GCase, were obtained from IMR90 fibroblasts (human lung fibroblasts, ATCC-CCL-186). For this purpose, fibroblasts were grown to confluence in 100 mm dishes using DMEM high glucose medium (Invitrogen) supplemented with antibiotics (100 U/mL penicillin/streptomycin, Gibco)

and 10% fetal bovine serum (FBS, Gibco) at 37 ºC in a 5% CO_2 humidified atmosphere. Cells from each plate were detached with 1 mL of trypsin (0.05% trypsin/EDTA, Invitrogen) for 10 min at 37 ºC and 4 mL of fresh medium were added to re-suspend the cells. The concentration of cells was determined by counting in a Neubauer camera using trypan blue as a vital stain. For the biological assays, cells from three plates were transferred to a 50 mL conical tube and centrifuged (10 min, 300×g), washed with PBS and centrifuged again. Cells were then re-suspended with 1 mL of PBS, counted, aliquoted and transferred to an Eppendorf tube and centrifuged (5 min, 600×g). The final cell pellet was frozen in liquid nitrogen and stored at –80 ºC until use.

Cell lysates were obtained from the harvested IMR90 fibroblasts. Aliquots of 10.7×10^6 cell pellets (each coming from three 100-mm dishes) were homogenized with 450 µL of lysis buffer (100 mM NaCl, 1 mM $MgCl_2$, 0.2% Triton X-100 (v/v), 10 mM HEPES, pH 7.4) containing 1 µg/ml aprotinin, 1 µg/ml leupeptin and 0.1 mM PMSF as protease inhibitors. Cells were broken by 20 strokes using an Eppendorf pestle and left on ice for 15 min. Cell debris was removed by centrifugation (600×g, 5 min, 4 °C) and the supernatant was aliquoted, frozen in liquid nitrogen and stored at –80 ºC.

To check the activity of the AH released from the electrospun MFs and multilayered devices, a modification of the thermal denaturation and enzyme activity assays described by Diettrich *et al.*[17] and Maegawa *et al.*[3] was used. Briefly, cell lysates (23 µL) were incubated for 60 min at 50 °C with one volume of PBS either with or without AH (fresh or released from PCL-based systems). Samples were then kept on ice for 5 min and left to equilibrate at room temperature for 5 more minutes. The same procedure using samples not submitted to thermal denaturation (kept on ice) was also carried out as a control. All the samples were prepared by duplicate.

GCase activity of the samples was tested using the fluorogenic substrate 4-methylumbelliferyl-β-D-glucopyranoside, MUbGlc (Sigma). To do this, one volume (46 μL) of substrate solution (12 mM MUbGlc, 50 mM sodium taurocholate, 0.2% Triton X-100 v/v, 0.2% human serum albumin w/v, 40 mM $CaCl_2$ in McIlvaine's citrate-phosphate buffer, pH 5.40) was added to each sample. After incubation for 1 h at 37 ºC, the reaction was stopped by adding 2.5 volumes of stop solution (0.25 M Glycine/NaOH buffer, pH 10.5). Samples were placed in a 96-well black plate (300 μL/well) and the fluorescence from the 4-methylumbelliferone (MU) reporter group released after hydrolysis of the substrate was measured in a microplate spectrofluorometer (Synergy HTX multimode reader, BioTek) with the excitation wavelength set at 360 nm and the emission wavelength at 460 nm. The relative remaining activity of GCase after thermal denaturation was calculated by comparison with the activity measured for the corresponding control samples kept on ice (*i.e.* not submitted to thermal denaturation).

3. Results and discussion

3.1. Preparation and characterization of AH-loaded fibers

Mixtures of PCL dissolved in chloroform:acetone and AH dissolved in TFE or FA were electrospun to obtain PCL/AH(TFE) or PCL/AH(FA) MFs, respectively. The wt % of AH used in the feeding solution, which was identical in both cases, was completely incorporated into the PCL matrix during the electrospinning process. Figure 1 compares SEM micrographs and diameter distributions of PCL/AH(TFE) and PCL/AH(FA) MFs obtained after optimization of the electrospinning conditions with those of unloaded PCL(TFE) and PCL(FA) control samples.

The utilization of TFE and FA resulted in the formation of well-defined MFs, in which droplets and beads were not detected. However, the morphology was seriously affected by both the incorporation of the drug into the polyester matrix and the effect of the solvent used to dissolve the PC in the viscosity of the feeding solution. More specifically, PCL/AH(FA) MFs present a cylindrical morphology with an average diameter (*D*) of 717±32 nm, while PCL/AH(TFE) MFs are much flatter, exhibiting a ribbon-like morphology and similar diameter (*D*= 694±13 nm). Both unloaded PCL(TFE) and PCL(FA) fibers exhibited cylindrical morphology, evidencing that, in spite of its low concentration, the influence of the PC in the viscosity of the feeding solution is much higher when it is dissolved in TFE than in FA. Clearly, this is due to the amount of TFE in the feeding solutions used to prepare PCL/AH(TFE) and PCL(TFE), which is almost 30 times greater than the amount FA in the solutions employed to electrospun PCL/AH(FA) and PCL(FA). The remarkable influence of the TFE solvent on the viscosity of the feed solution is confirmed by the diameter of PCL(TFE) MFs (*D*= 1488±88 nm), which is more than twice that of PCL(FA) MFs (*D*= 633±33 nm).

Interestingly, PCL/AH(TFE) and PCL/AH(FA) show well-adhered particles homogeneously distributed along surface of the MFs (Figure 1). These round-like particles, which exhibit a diameter of several hundred of nanometers and ~100 nm for PCL/AH(TFE) and PCL/AH(FA), respectively, have been assigned to crystallized AH. These results have been attributed to the influence of AH···solvent interactions during the electrospinning process. Thus, the drug, which bears polar groups, forms crystalline domains that remain at the surface of hydrophobic PCL MFs when the electrospinning process causes the elimination of favorable AH···solvent interactions.[18] Moreover, the flat ribbon-like geometry of PCL/AH(TFE) fibers is probably due to the influence of

unfavorable PCL···AH interactions in the chain entanglement of the solution mixture.[18] Thus, both the incorporation of a low molecular weight drug and the formation of such PCL···AH interactions decrease the degree of chain entanglement in the feeding solution, which is a parameter that significantly influence the fiber morphology.

AFM height and phase-contrast images are displayed in Figure 2 for all electrospun MFs, 3D topographic images being additionally included for PCL/AH(TFE) and PCL/AH(FA). AFM images are fully consistent with previously discussed SEM observations. Both AH-loaded and unloaded MFs present a very smooth surface, the roughness ranging from R_q= 6±2 nm for PCL/AH(TFE) to 16±3 nm for PCL(FA). Furthermore, AFM phase-contrast images obtained for PCL/AH(TFE) and PCL/AH(FA) allow to distinguish two materials with different elastic properties, which have been associated to the AH aggregates and the PCL matrix. This observation, which is much clearer for PCL/AH(TFE) than for PCL/AH(FA) due to the different sizes of AH aggregates, supports that the polar drug organizes in microphases separated from the non-polar polyester matrix.

In order to corroborate that AH was successfully loaded in the PCL MFs, FTIR, Raman and UV-vis spectroscopic studies were conducted. Unfortunately, the FTIR spectra recorded for AH-loaded MFs were practically identical to the spectrum of unprocessed PCL powder and, therefore, the characteristic bands associated to the drug were undistinguishable (Figure S2). On the other hand, Figures 3a and 3b display the Raman spectra of electrospun MFs obtained using TFE and FA solvents, respectively. The spectrum of AH is included in both graphics for comparison. In addition to the bands observed for unloaded PCL, the spectra of AH-loaded MFs present some bands that have been associated to the PC. The weak bands at 1590 and 1555 cm^{-1}, which are

detected in the spectra of both PCL/AH(TFE) and PCL/AH(FA), have been attributed to the primary and secondary amines of AH (Scheme 1), respectively.[19] Besides, the weak signals observed at around 800 cm^{-1} in the PCL/AH(TFE) spectrum have been related with the Ar-Br Raman active modes,[19] even though these are practically undetectable for PCL/AH(FA).

The presence of AH in loaded MFs was also investigated by UV-vis spectroscopy. For this purpose 1×1 cm^2 samples were cut from AH-loaded fibrous mats and dissolved in chloroform. Then, the PC was extracted using water, as described in the Methods section. UV-vis spectra of four different AH-containing aqueous solutions derived from PCL/AH(TFE) fibrous mats are displayed in Figure 3c together with the quantification of the PC. All spectra showed an absorption band at 307 nm, even though its intensity differs from sample to sample. Although the presence of the band confirms the successful loading of AH, the dispersion in the quantified value, with an average value of 1.54±0.64 *w*/*w*%, reflects that the drug is heterogeneously distributed in the PCL matrix. Similar results were observed in the spectra recorded from PCL/AH(FA) mats (Figure S3), the average content being in this case 1.55±0.81 *w*/*w*%. AH loading is further supported by the XPS atomic compositions obtained for the different studied MFs, which are compared in Table 1. Both N and Br are detected in PCL/AH(TFE) and PCL/AH(FA), while these atoms are absent in PCL(TFE) and PCL(FA).

The water contact angle (θ) of fibrous mats was determined for AH-loaded and unloaded PCL matrixes (Figure 3d). The contact angles indicate that all materials are hydrophobic (*i.e.* $\theta > 90^{o}$) and, interestingly, the wettability does not change upon the incorporation of the polar PC. This behavior can be explained by the combination of three factors: *i*) the PCL matrix is hydrophobic; *ii*) the concentration of AH in the loaded fibers is very small; and *iii*) the micro-nanopatterned structure on the surface of

the mat. Regarding to the latter, the micrometric diameter of the electrospun fibers (*i.e.* 0.6-1.5 μm in Figure 1) combined with the nanometric roughness (*i.e.* 8-16 nm in Figure 2) and holes among neighboring fibers favor the entrapment of air, which may give place to a Cassie Baxter stable state.[20]

3.2. Release from loaded fibers

AH release from loaded electrospun MFs is expected to depend on the relative strength of the interactions between the drug and the PCL matrix or the molecules from the release medium (*i.e.* water and ions). AH-loaded and unloaded (negative control) fibrous mats were immersed in PBS using Eppendorf tubes, as described in the Methods section. At regular time intervals (*i.e.* 5, 15, 30, 45, 60, 90, 120, 360, 1440 min), release medium (1 mL) was withdrawn from the tube, replaced by 1 mL of fresh medium, and analyzed by UV-vis spectroscopy. The amount of AH released to the medium was quantified using the band centered at 307 nm, which corresponds to the PC.

Figure 4a compares the UV-vis spectra of the released media extracted after 5, 15, 30 and 60 min from samples consisting of PCL/AH(TFE) mats immersed in PBS. The content of AH in the release medium was high at the beginning and decreased very rapidly with time (*i.e.* from 1.59 *w*/*w* % after 5 min to 0.06 *w*/*w* % after 60 min), evidencing a very fast release. Accordingly, the release curve (Figure 4b) indicates that 80% of the PC was released to the PBS medium during the first 15 min, whereas the amount of AH that remained in the MFs after 6 h was lower than < 1%. The behavior of samples from PCL/AH(FA) mats immersed in PBS was practically identical, as reflected in the UV-vis spectra and the release curve displayed in Figures S4a-b. The very fast release in PBS has been associated to the weakness of AH···PCL interactions, which are expected to be rapidly compensated by the strong interactions between the

polar groups of AH and the components of PBS medium. In order to enhance the efficiency of therapies based on the controlled release of polar drugs, the fast mechanism observed for loaded PCL MFs requires modification into an extended release mechanism. For this purpose, in the following sub-sections we first demonstrate the activity of the released AH and, then, we show how different coating strategies allow to delay and regulate the drug release dosage.

3.3. Activity of released AH

Many lysosomal storage disorders (LSDs) originate from mutations that affect the proper folding of the enzyme in the ER. PCs allow mutant enzymes to be correctly folded, thus avoiding endoplasmic reticulum retention and granting their transportation to the lysosomes, where the enzyme–PC complex dissociates due to the low pH and high substrate concentration.[21] Specifically, AH has been reported to be an excellent PC candidate for Gaucher disease, which is the most common autosomal recessive LSD.[3,22] Gaucher disease is caused by mutations in the gene encoding lysosomal GCase and ultimately resulting in the accumulation of glucosylceramide in macrophages and the development of hepatosplenomegaly, anaemia, skeletal lesions and central nervous system dysfunctions.[23]

Previous studies pointed to the efficacy of AH in increasing GCase activity[3,6] and thermal stability.[3,22] In this section, we examine if AH maintains this stabilizing activity once released from loaded electrospun PCL MFs. For this purpose, a thermal denaturation assay utilizing GCase from lysed fibroblasts was conducted in the absence or in the presence of both fresh and released AH (see Methods section). Residual GCase activity after thermal denaturation was standardized by comparison with the GCase activity obtained from the sample that was kept at 0 ºC (non-denaturation control).

Enzyme activity was evaluated by measuring the fluorescence resulting from the release of the fluorescent reporter 4-MU group from the substrate. Thus, the remaining activity in the presence of either fresh or released AH was obtained dividing the fluorescence measured for the thermally denatured samples by the fluorescence of the corresponding sample kept at 0 ºC.

Figure 4c compares the remaining activity of GCase after thermal denaturation in the presence of the AH released from PCL/AH(TFE) and PCL/AH(FA) MFs after 5 min in PBS, fresh AH in PBS, and PBS alone (without AH). Results show the protecting effect on GCase activity of AH, which is in agreement with the reported literature.[3] Thus, all the samples of GCase that have been submitted to heating in the presence of AH (either fresh or released from the fibers) show more activity than the enzyme sample heated without AH being present. Moreover, the GCase activity is slightly higher in the presence of AH released from MFs than with fresh AH, showing that the functionality of the PC is not damaged by the aggressive conditions of the electrospinning process. These results indicate that PCL is a suitable vehicle to encapsulate biactive polar drugs such as AH and, thus, improvement of the release mechanism to obtain a gradual dosage deserves consideration.

3.4. Regulating the AH release by applying coating strategies

In order to delay the delivery of the PC, two different coating approaches were examined. In the first one, PCL/AH(TFE) and PCL/AH(FA) fibrous mats were sandwiched between two spin-coated PCL NMs. The process used to prepare these 3-layered NM/MFs/NM systems, hereafter denoted PCL//PCL/AH(TFE)//PCL and PCL//PCL/AH(FA)//PCL, respectively, is summarized in Figure 5a. Free-standing sandwiched systems were prepared by spin-coating a PCL NM onto a Teflon® substrate

using an acetone polymer solution (see Methods). Then, a 1 cm^2 PCL/AH(TFE) or PCL/AH(FA) square piece, which was cut from the corresponding fibrous mat, was put onto the first PCL NM and the second PCL NM was spin-coated onto it. Finally, the sandwiched system was easily detached from the Teflon® substrate. It is worth noting that the solubility of PCL in acetone is very slow, especially with respect to chloroform or chloroform:acetone mixtures, which allowed to minimize the attack of the solvent to the PCL MFs during the spin-coating process. Sandwiched systems using unloaded PCL(TFE) and PCL(FA) fibrous mats were also prepared as controls for release assays. Sandwiched systems supported onto the Teflon® substrate were employed for SEM characterization.

In the second coating strategy, AH-loaded fibrous mats were modified through a dip-coating method, as schematically described in Figure 5b. More specifically, 1×1 cm^2 PCL/AH(TFE) and PCL/AH(FA) square pieces were immersed in a solution of PCL in acetone for 3 s. The resulting samples, hereafter denoted PCL[PCL/AH(TFE)] and PCL[PCL/AH(FA)], were dried and used for release assays. Control samples were prepared using unloaded fibrous mats.

SEM micrographs of the bottom PCL NM and the two sandwiched systems are displayed in Figure 6a. The bottom PCL NM presents a very flat, homogeneous and smooth surface, the thickness being of only 747±85 nm. In contrast, the shape of the top PCL layer adapts to the ribbon-like and the cylindrical morphology of PCL/AH(TFE) and PCL/AH(FA) MFs, respectively, acting as a coating. It is worth noting that, in the latter case, the top PCL NM wraps perfectly the MFs and the only fingerprint of its presence corresponds to the pseudo-periodic folds that systematically appears in the direction perpendicular to the fiber axis. These folds can be associated to the effect of the acetone used to dissolve PCL. In contrast, the PCL NM spin-coated onto

PCL/AH(TFE) MFs exhibits a heterogeneous aspect. In these samples, regions involving wrapped MFs with the previously described folds coexist with small areas in which the structure of the MFs is no longer distinguishable, which is probably due to the flat morphology of the ribbon-like PCL/AH(TFE) MFs.

SEM micrographs of PCL[PCL/AH(TFE)] and PCL[PCL/AH(FA)] are displayed in Figure 6b. Although the morphologies of the latter systems are apparently similar to those obtained for PCL//PCL/AH(TFE)//PCL and PCL//PCL/AH(FA)//PCL, detailed inspection evidences important differences. For example, PCL[PCL/AH(FA)] shows a heterogeneous structure in which neighboring MFs are partially joined by irregular portions of films formed after solvent evaporation, while these elements are imperceptible in PCL[PCL/AH(TFE)]. In contrast, the density of folds is much lower at the surface of PCL[PCL/AH(TFE)] than at the surface of all the other coated systems. Overall, these differences indicate that the dip-coating technique is much more influenced by the morphology of the MFs than the spin-coating.

The water contact angle of fibrous mats coated with PCL by spin-coating and dip-coating are displayed in Figures S5 and S6, respectively. The measured contact angles ranged from 85º to 99º, evidencing a significant reduction with respect to uncoated fibrous mats (Figure 3d). This reduction has been attributed to the fact that the external coating eliminates the micro-nanopatterned structure found on the surface of the fibrous mats. Thus, the PCL coating dominates the wettability of the new scaffolds, which exhibit in all cases contact angles close to the lowest threshold of hydrophocity (*i.e.* $\theta >$ 90º).

Figure 7 compares the release profiles of AH-loaded systems prepared by spin-coating and dip-coating. The release was very slow in all cases, even though with some differences. For example, a release percentage of 95% was reached after ~2 and ~1

months of exposure to the medium for sandwiched and dip-coated systems, respectively, while the time required by uncoated MFs was only ~1 h. Accordingly, the coating has a very significant impact in the kinetics of the release. Moreover, the extent of the delay in the release of the PC largely depends on the technique used to protect the MFs. The delay is much longer when fibrous mats are sandwiched between two spin-coated NMs than when coated through simple immersion in a PCL solution. Indeed, the effect of the coating technique is observed even in the first steps of the release, as evidenced in the insets displayed in Figure 7. Thus, the release profiles obtained for PCL//PCL/AH(TFE)//PCL and PCL//PCL/AH(FA)//PCL are very similar for both short and large times of exposure, which indicate that the protection imparted by homogeneous spin-coated NMs does not depend on the morphology of the fibrous mats. In contrast, the profiles obtained for PCL[PCL/AH(TFE)] and PCL[PCL/AH(FA)] present important differences, especially for short times (*e.g.* after 6 h of exposure the release percentage was 64% and 42% for the former and the latter, respectively). These differences are attributed to the heterogeneous structure of the systems prepared by dip-coating (Figure 6), which is apparently affected by the morphology of the MFs.

Figure 8 compares the time required to release 50% and 80% of loaded AH from all the studied systems. A it was expected, the delivery of coated systems was clearly delayed with respect to that observed from the MFs alone since AH had to diffuse through the PCL coats. However, the most remarkable result displayed in Figure 8 is that it demonstrates that the AH release can be regulated through the morphology of the scaffold without changing the composition of the PCL matrix. Thus, the time required for release can extend from a few minutes for uncoated MFs to few days or almost a week for dip-coated or sandwiched systems, respectively.

4. Conclusion

The present study reveals that AH, a small and polar PC that increases the activity of misfolded GCase, can be loaded in fibrous PCL scaffolds by electrospinning. The fast release rate of this drug from such fibrous scaffolds, which occurs in less than an hour, has been controlled by applying external coatings to the MFs. These coatings, which have been achieved by dip-coating and by spin-coating, have been obtained using PCL dissolved in acetone to avoid the rapid dissolution of the AH-loaded MFs. The AH release extends to weeks and months when coated fibrous scaffolds are prepared by dip-coating and spin-coating, respectively. The released AH retains the protecting effect on the activity of GCase, demonstrating that the electrospinning process does not affect the functionality of the drug. Moreover, PCL coated-fibrous scaffolds can be used to regulate strategically the dosage of polar drugs depending on the therapeutic needs.

Acknowledgements

Authors acknowledge MINECO/FEDER (MAT2015-69367-R and MAT2015-69547-R), Agència de Gestió d'Ajuts Universitaris i de Recerca (2017SGR359 and 2017SGR373) for financial support. Support for the research of C.A. was received through the prize “ICREA Academia” for excellence in research funded by the Generalitat de Catalunya. Dr. E. Armelin, Dr. J. Guillem, Dr. M. P. Almajano and Mr. J. Sans are thanked for their assistance and suggestions in some experiments.

References

[1] a) N. Gregersen, P. Bross, S. Vang, J. H. Christensen, *Annu. Rev. Genomics Hum. Genet.* **2006**, *7*, 103; b) F. U. Hartl, *Annu Rev Biochem.* **2017**, *86*, 21; c) E. Herczenik,

M. F. B. G. Gebbink, *FASEB J.* **2008**, *22*, 2115; d) P. Leandro, C. M. Gomes, *Mini Rev. Med. Chem.* **2008**, *8*, 901.

[2] a) G. Parenti, G. Andria, K. J. Valenzano, *Mol Ther.* **2015**, *23*, 1138; b) G. Parenti, C. Pignata, P. Vajro, M. C. Salerno**,** *Int. J. Mol. Med.* **2013**, *31*, 11; c) K. J. Valenzano, R. Khanna, A. C. Powe, R. Boyd, G. Lee, J. J. Flanagan, E. R. Benjamin, *Assay Drug Dev. Technol.* **2011**, *9*, 213; d) G. Parenti, *EMBO Mol. Med.* **2009**, *1*, 268; e) A. Banning, C. Gülec, J. Rouvinen, S. J. Gray, R. Tikkanen, *Sci Rep.* **2016**, *23*;6:37583; f) G. Parenti, G. Andria, A. Ballabio, *Annu Rev. Med.* **2015**, *66***,** 471; g) R. E. Boyd, *J. Med. Chem.* **2013**, *56***,** 2705.

[3] G. H. B.Maegawa, M. B. Tropak, J. D. Buttner, B. A. Rigat, M. Fuller, D. Pandit, L. Tang, G. J. Kornhaber, Y. Hamuro, J. T. R. Clarke, D. J. Mahuran, *J. Biol. Chem.* **2009**, *284*, 23502.

[4] a) A. McNeill, J. Magalhaes, C. Shen, K.-Y. Chau, D. Hughes, A. Mehta, T. Foltynie, J. M. Cooper, A. Y. Abramov, M. Gegg, A. H. V. Schapira, *Brain J. Neurol.* **2014**, *137*, 1481; b) G. Babajani, M. B. Tropak, D. J. Mahuran, A. R. Kermode, *Mol. Genet. Metab.* **2012**, *106*, 323; c) M. M. Ivanova, E. Changsila, A. Turgut, O. Goker-Alpan, *Am. J. Transl. Res.* **2018**, *10*, 3750.

[5] a) Z. Luan, L. Li, K. Higaki, E. Nanba, Y. Suzuki, K. Ohno, *Brain Dev.* **2013**, *35*, 317; b) T. Suzuki,M. Shimoda, K. Ito, S. Hanai, H. Aizawa, T. Kato, K. Kawasaki, T. Yamaguchi, H.D. Ryoo, N. Goto-Inoue,M. Setou, S. Tsuji, N. Ishida, *PLoS One* **2013**, *8*, e69147.

[6] A. Narita, K. Shirai, S. Itamura, A. Matsuda, A. Ishihara, K. Matsushita, C. Fukuda, N. Kubota, R. Takayama, H. Shigematsu, A. Hayashi, T. Kumada, K. Yuge, Y. Watanabe, S. Kosugi, H. Nishida, Y. Kimura, Y. Endo, K. Higaki, E. Nanba, Y.

Nishimura, A. Tamasaki, M. Togawa, Y. Saito, Y. Maegaki, K. Ohno, Y. Suzuki, *Ann. Clin. Transl. Neurol.* **2016**, *3*, 200.

[7] a) M. Staples, *Wiley Interdiscip. Rev.: Nanomed. Nanobiotechnol.* **2010**, *2*, 400; b) B. P. Timko, D. S. Kohane, *Clin. Ther.* **2012**, *34*, S25.

[8] S. Mura, J. Nicolas, P. Couvreur, *Nat. Mater.* 2013, **12**, 991.

[9] a) B. P. Timko, T. Dvir, D. S. Kohane, *Adv. Mater.* **2010**, *22*, 4925; b) A. Puiggalí-Jou, P. Micheletti, F. Estrany, L. J. del Valle, C. Alemán, *Adv. Healthc. Mater.* **2017**, *6* 1700453; c) S. Merino, C. Martin, K. Kostarelos, M. Prato, E. Vázquez, *ACS Nano* **2015**, *9* 4686; d) N. S. Satarkar, D. Biswal, J. Z. Hilt, *Soft Matter* **2010**, *6*, 2364.

[10] A. Puiggalí-Jou, A. Cejudo, L. J. del Valle, C. Alemán, *ACS Appl. Bio Mater.* **2018**, *1*, 1594.

[11] a) D.H. Reneker, I. Chun, *Nanotechnology* **1996**, *7*, 216; b) A. Frenot, I.S. Chronakis, *Curr. Opin. Colloid Interface Sci*. **2003**, *8*, 64; c) Y. Dzenis, *Science* **2004**, *304*, 1917; d) K. Jayaraman, M. Kotaki, Y. Zhang, X. Mo, S. Ramakrishna, *J. Nanosci. Nanotechnol.*, **2004**, *4*, 52.

[12] a) S. R. Dhakate, B. Singla, M. Uppal, R. B. Mathur, Adv. Mater. Lett. **2010**, *1*, 200; b) S. Sharma, Adv. Mater. Lett. **2013**, *4*, 522.

[13] X. Liu, Y. Yang, D.-G. Yu, M.-J. Zhu, M. Zhao, G. R. Williams, *Chem. Eng. J.* **2018**, *292*, 886; b) D. G. Yu, G. R. Williams, M. Zhao, *J. Control. Release* **2018**, *292*, 91.

[14] a) T. Hai, X. Wan, D.-G. Yi, K. Wang, Y Yang, Z.-P. Liu, *Mater. Des.* **2019**, *162*, 70; b) Y. Yang, W. Li, G. Wang, G. R. Williams, Z. Zhang, *Carbohydr. Polym.* **2019**, *203*, 228.

[15] a) M. A. Woodruff, D. W. Hutmacher, *Prog. Polym. Sci.* **2010**, *35*, 1217; b) R. H. Dong, Y. X. Jia, C. C. Qin, L. Zhan, X. Yan, L. Cui, Y. Zhou, X. Jiang, Y. Z. Long,

Nanoscale **2016**, *8*, 3482; c) L. J. del Valle, R. Camps, A. Díaz, L. Franco, A. Rodríguez-Galán, J. Puiggalí. *J. Polym. Res.* **2011**, *18*, 1903.

[16] L. A. Bosworth, S. Downes. *J. Polym. Environ.* **2012**, *20*, 879.

[17] O. Diettrich, K. Mills, A. W. Johnson, A. Hasilik, B. G. Winchester, *FEBS Lett.* **1998**, *441*, 369.

[18] S. Maione, M. M. Pérez-Madrigal, L. J. del Valle, A. Díaz, L. Franco, C. Cativiela, J. Puiggalí, C. Alemán, *J. Appl. Polym.* Sci. **2017**, *134*, 44883

[19] Infrared and Raman Characteristic Group Frequencies: Tables and Charts, 3rd edition, G. Socrates, John Wiley & Sons Ltd, West Sussex, England, 2001.

[20] a) S. Moradi, S. Kamal, P. Englezos, S. G. Hatzikiriakos, *Nanotechnology* **2013**, *24*, 415302; b) E. Armelin, S. Moradi, S. G. Hatzikiriakos, C. Alemán, C. *Adv. Eng. Mater.* **2018**, *20*, 1700814.

[21] D. M. Pereira, P. Valentão, P. B. Andrade, *Chem. Sci.* **2018**, *9*, 1740.

[22] J. Aymami, X. Barril, L. Rodríguez-Pascau, M. Martinell, *Pharm. Pat. Anal.* **2013**, *2*, 109.

[23] A. S. Thomas, A. Mehta, D. A. Hughes, *Br. J. Haematol.* **2014**, *165*, 427.

Table 1. Atomic percent composition obtained by XPS for AH-loaded and unloaded PCL fibers.

	C	N	O	Br
PCL/AH(TFE)	81.81	0.19	17.95	0.05
PCL(TFE)	80.04	-	19.96	-
PCL/AH(FA)	81.77	0.12	18.08	0.03
PCL(FA)	82.32	-	17.68	-

CAPTIONS TO FIGURES

Figure 1. SEM micrographs taken at low (left) and high (center) magnification for electrospun fibers of PCL/AH(TFE), PCL(TFE), PCL/AH(FA) and PCL(FA). The diameter distribution of the electrospun microfibers and the corresponding average value ± standard deviation are displayed at the right. Particles adhered to the surface of the PCL matrix, which have been associated to the crystallized drug, are marked by red boxes for PCL/AH(TFE) and PCL/AH(FA).

Figure 2. AFM images of PCL/AH(TFE), PCL(TFE), PCL/AH(FA) and PCL(FA): 2D height (left), 3D topographic (center; only for AH-loaded MFs) and phase-contrast (right) images. The root mean square roughness (R_q) is displayed for each system.

Figure 3. Comparison between the Raman spectra recorded for: (a) PCL/AH(TFE), PCL(TFE) and AH; and (b) PCL/AH(FA), PCL(FA) and AH. The weak peaks associated to AH in the spectra of PCL/AH(TFE) and PCL/AH(FA) are marked by the colored bars. (c) UV-vis spectra of the AH-containing water solutions extracted from four samples of PCL/AH(TFE) MFs dissolved in chloroform (left) and quantification of the AH contained in the extraction medium (right). The spectra corresponding to the PCL/AH(FA) mats are displayed in Figure S3. (d) Contact angle for water of PCL/AH(TFE), PCL(TFE), PCL/AH(FA) and PCL(FA) fibrous mats.

Figure 4. (a) UV-vis spectra of the PBS release media withdrawn at selected time intervals from Eppendorf tubes containing samples of PCL/AH(TFE). (b) AH release profile in PBS from PCL/AH(TFE) MFs. Complete description of the procedure employed for the release assays is provided in the Methods section. Results obtained for PCL/AH(FA) MFs are displayed in Figure S4. (c) Remaining GCase activity (%) (*i.e.* ratio between the enzymatic activity after thermal denaturation compared with the activity of the enzyme kept at 0 ºC) in the presence of AH released from PCL/AH(TFE)

and PCL/AH(FA) fibrous mats after 5 min immersed in PBS, fresh AH in PBS and without AH (PBS alone).

Figure 5. Procedure used to prepare: (a) free-standing PCL//PCL/AH(TFE)//PCL and PCL//PCL/AH(FA)//PCL by sandwiching the fibrous mat between two spin-coated PCL NMs; (b) Preparation of PCL[PCL/AH(TFE)] and PCL[PCL/AH(FA)] by dip-coating fibrous mats.

Figure 6. SEM micrographs of: (a) the PCL NM and the PCL//PCL/AH(TFE)//PCL and PCL//PCL/AH(FA)//PCL sandwiched systems obtained by spin-coating (Figure 5a). Representative regions in which the morphology of PCL/AH(TFE) MFs is lost are indicated by blue ellipsoids; (b) PCL[PCL/AH(TFE)] and PCL[PCL/AH(FA)] obtained by dip-coating (Figure 5b). Irregular portions of films joining neighboring MFs are indicated by yellow squares.

Figure 7. AH release profile in PBS from (a) sandwiched and (b) dip-coated systems.

Figure 8. Comparison of the time required to release 50% and 80% of the loaded AH from all the studied systems.

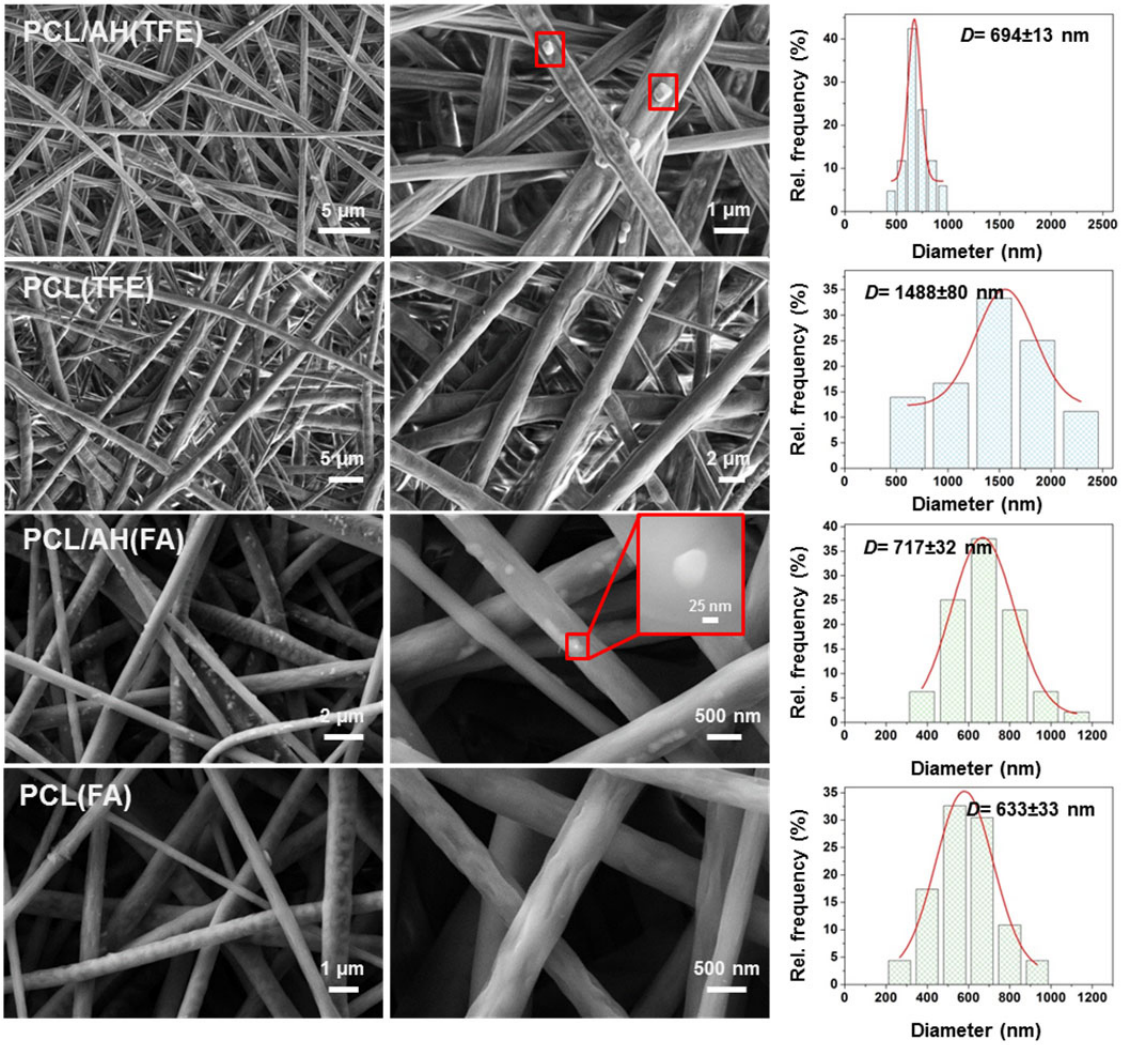
PCL/AH(TFE)
5 µm
1 µm
D= 694±13 nm
Rel. frequency (%)
Diameter (nm)
PCL(TFE)
5 µm
2 µm
D= 1488±80 nm
Rel. frequency (%)
Diameter (nm)
PCL/AH(FA)
2 µm
25 nm
500 nm
D= 717±32 nm
Rel. frequency (%)
Diameter (nm)
PCL(FA)
1 µm
500 nm
D= 633±33 nm
Rel. frequency (%)
Diameter (nm)

Figure 1

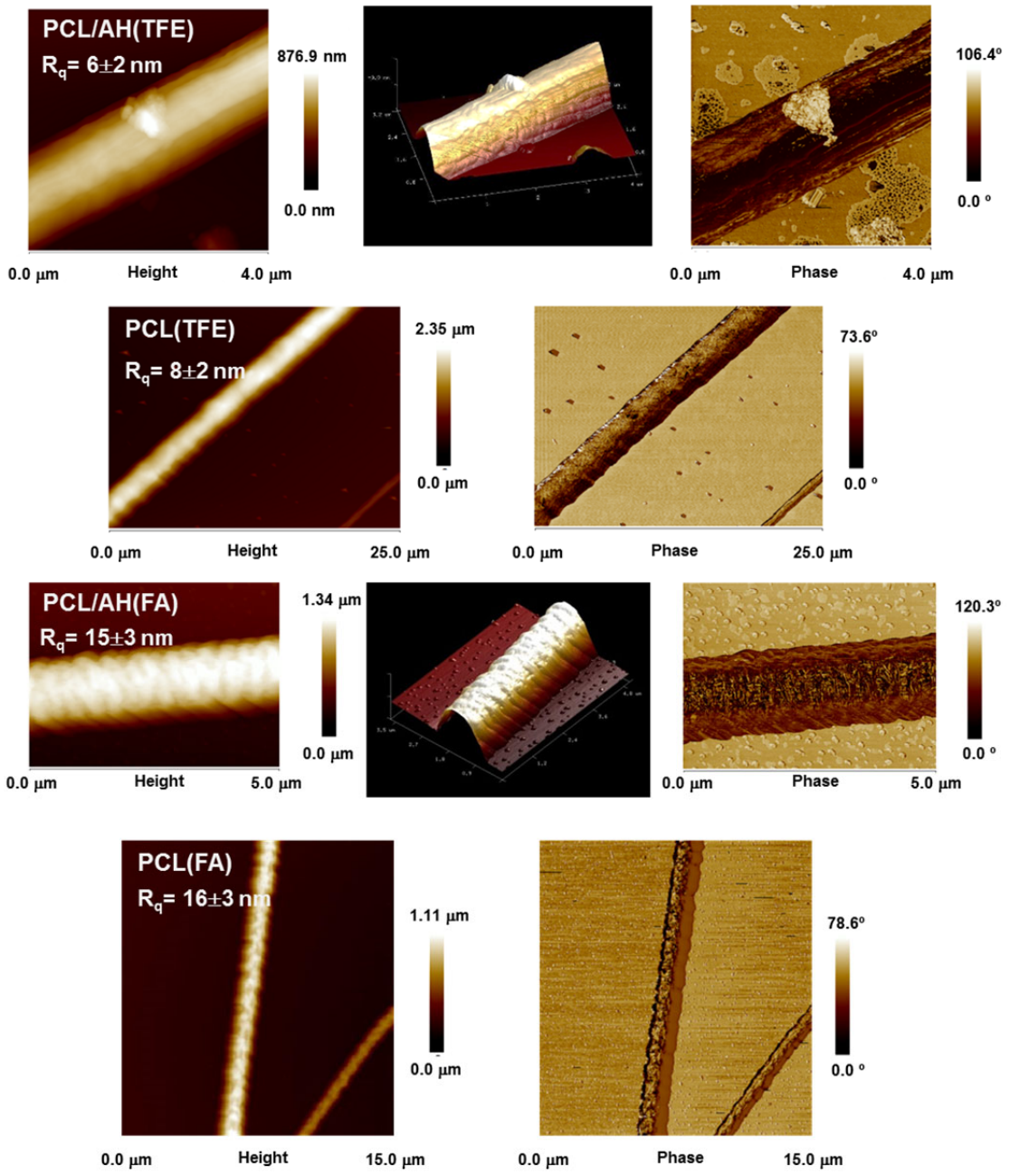
PCL/AH(TFE)
R_q= 6±2 nm
876.9 nm
0.0 nm
0.0 µm
Height
4.0 µm
106.4°
0.0 °
0.0 µm
Phase
4.0 µm
PCL(TFE)
R_q= 8±2 nm
2.35 µm
0.0 µm
0.0 µm
Height
25.0 µm
73.6°
0.0 °
0.0 µm
Phase
25.0 µm
PCL/AH(FA)
R_q= 15±3 nm
1.34 µm
0.0 µm
0.0 µm
Height
5.0 µm
120.3°
0.0 °
0.0 µm
Phase
5.0 µm
PCL(FA)
R_q= 16±3 nm
1.11 µm
0.0 µm
0.0 µm
Height
15.0 µm
78.6°
0.0 °
0.0 µm
Phase
15.0 µm

Figure 2

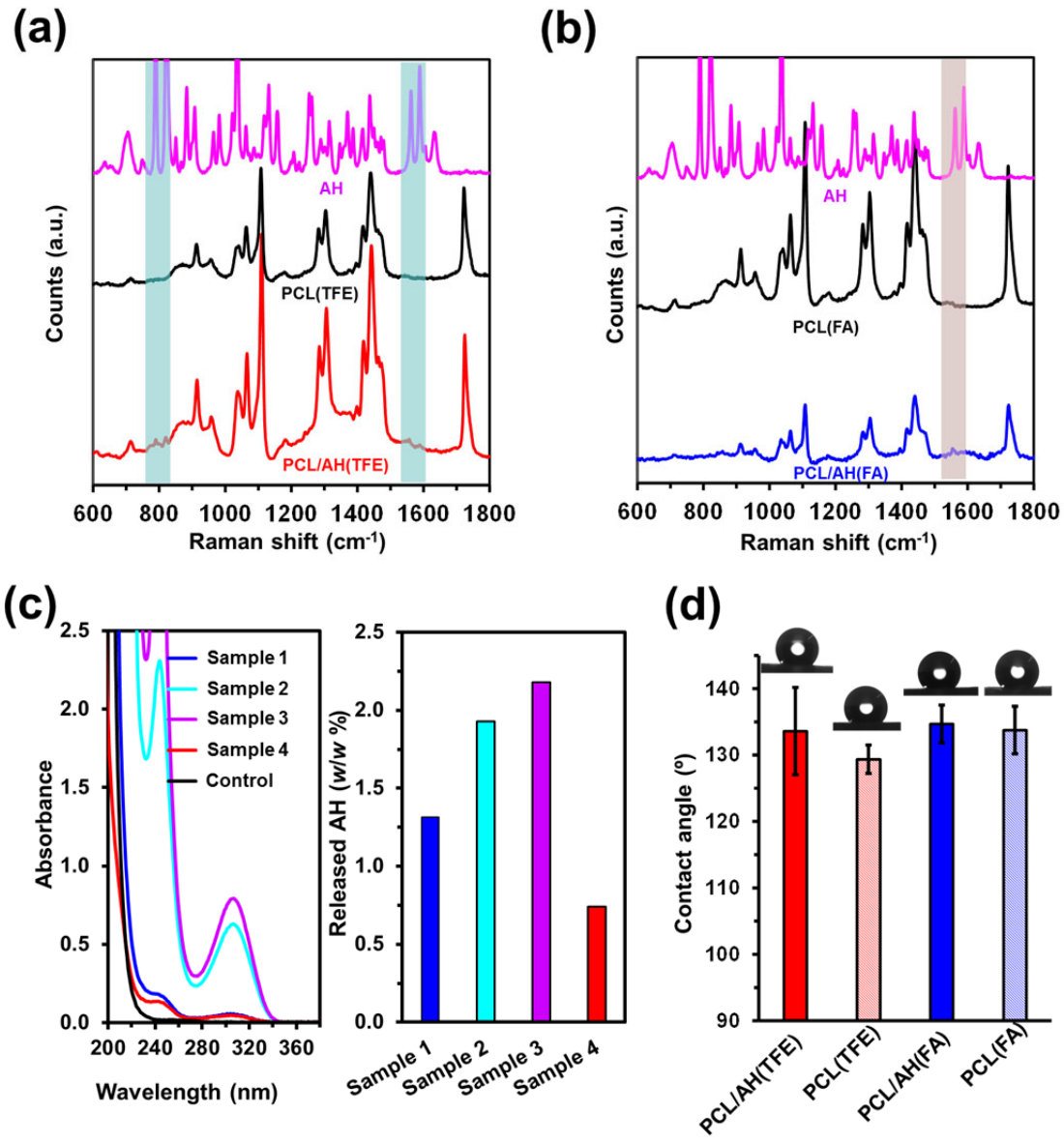
(a)
Counts (a.u.)
AH
PCL(TFE)
PCL/AH(TFE)
600 800 1000 1200 1400 1600 1800
Raman shift (cm-1)
(b)
Counts (a.u.)
AH
PCL(FA)
PCL/AH(FA)
600 800 1000 1200 1400 1600 1800
Raman shift (cm-1)
(c)
Absorbance
Sample 1
Sample 2
Sample 3
Sample 4
Control
200 240 280 320 360
Wavelength (nm)
Released AH (w/w %)
Sample 1
Sample 2
Sample 3
Sample 4
(d)
Contact angle (°)
PCL/AH(TFE)
PCL(TFE)
PCL/AH(FA)
PCL(FA)

Figure 3

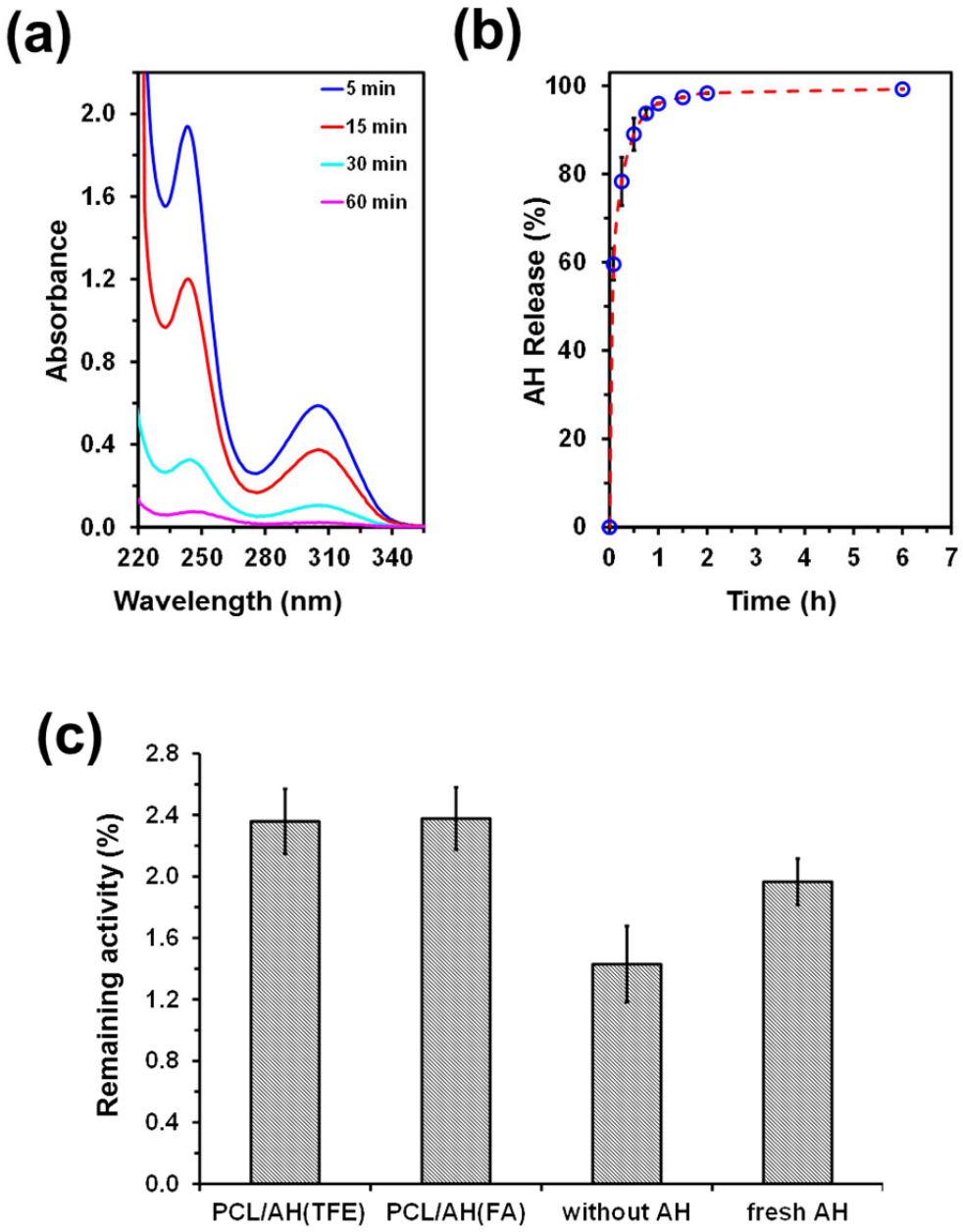
(a)
5 min
15 min
30 min
60 min
Absorbance
Wavelength (nm)
(b)
AH Release (%)
Time (h)
(c)
Remaining activity (%)
PCL/AH(TFE)
PCL/AH(FA)
without AH
fresh AH

Figure 4

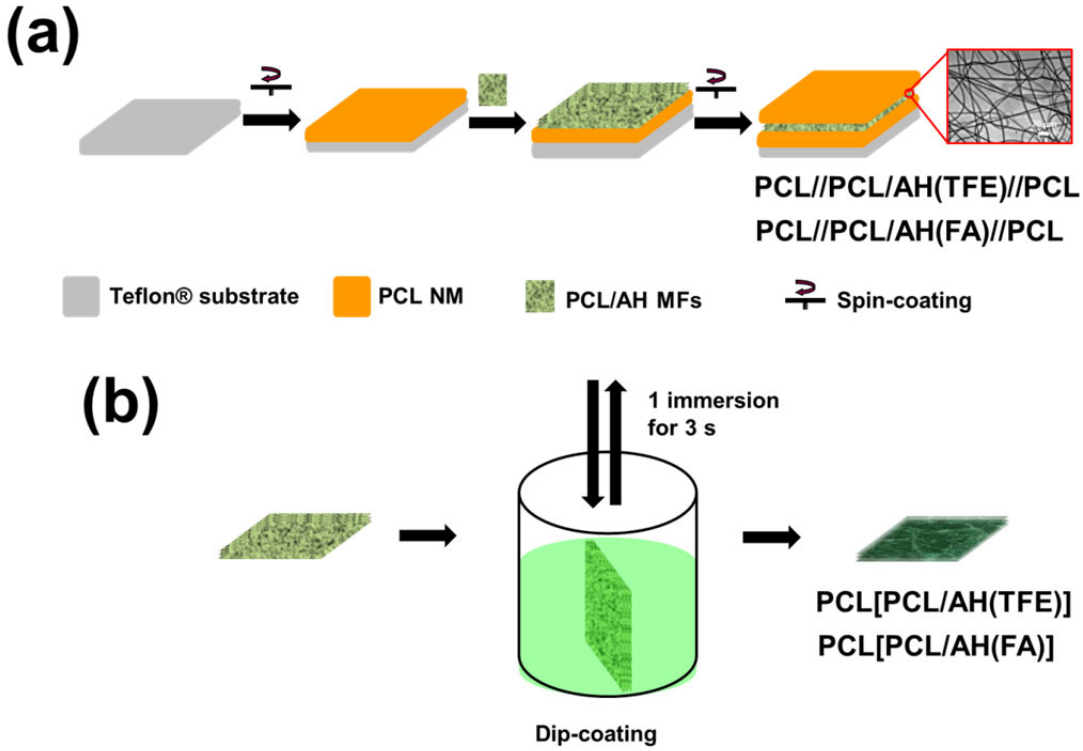
(a)
PCL//PCL/AH(TFE)//PCL
PCL//PCL/AH(FA)//PCL
Teflon® substrate
PCL NM
PCL/AH MFs
Spin-coating
(b)
1 immersion
for 3 s
PCL[PCL/AH(TFE)]
PCL[PCL/AH(FA)]
Dip-coating

Figure 5

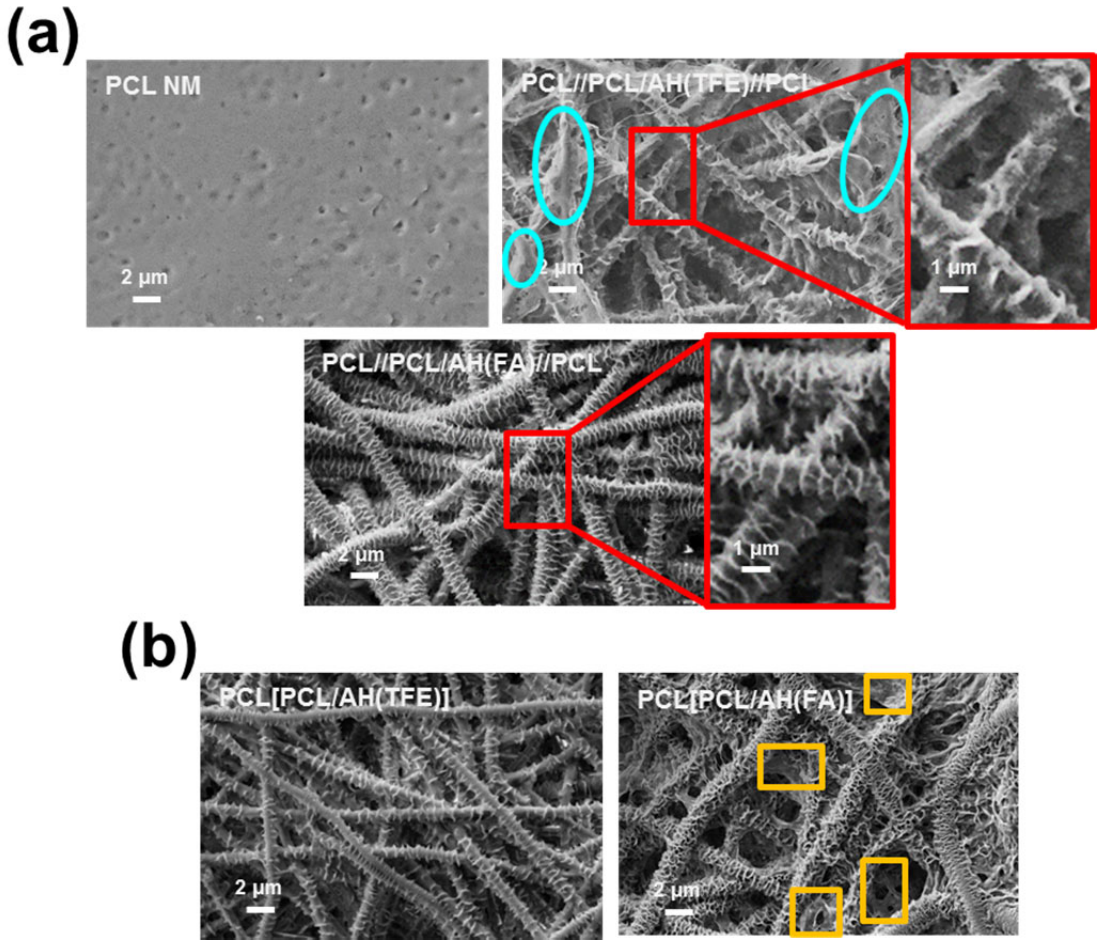
(a)
PCL NM
2 μm
PCL//PCL/AH(TFE)//PCL
2 μm
1 μm
PCL//PCL/AH(FA)//PCL
2 μm
1 μm
(b)
PCL[PCL/AH(TFE)]
2 μm
PCL[PCL/AH(FA)]
2 μm

Figure 6

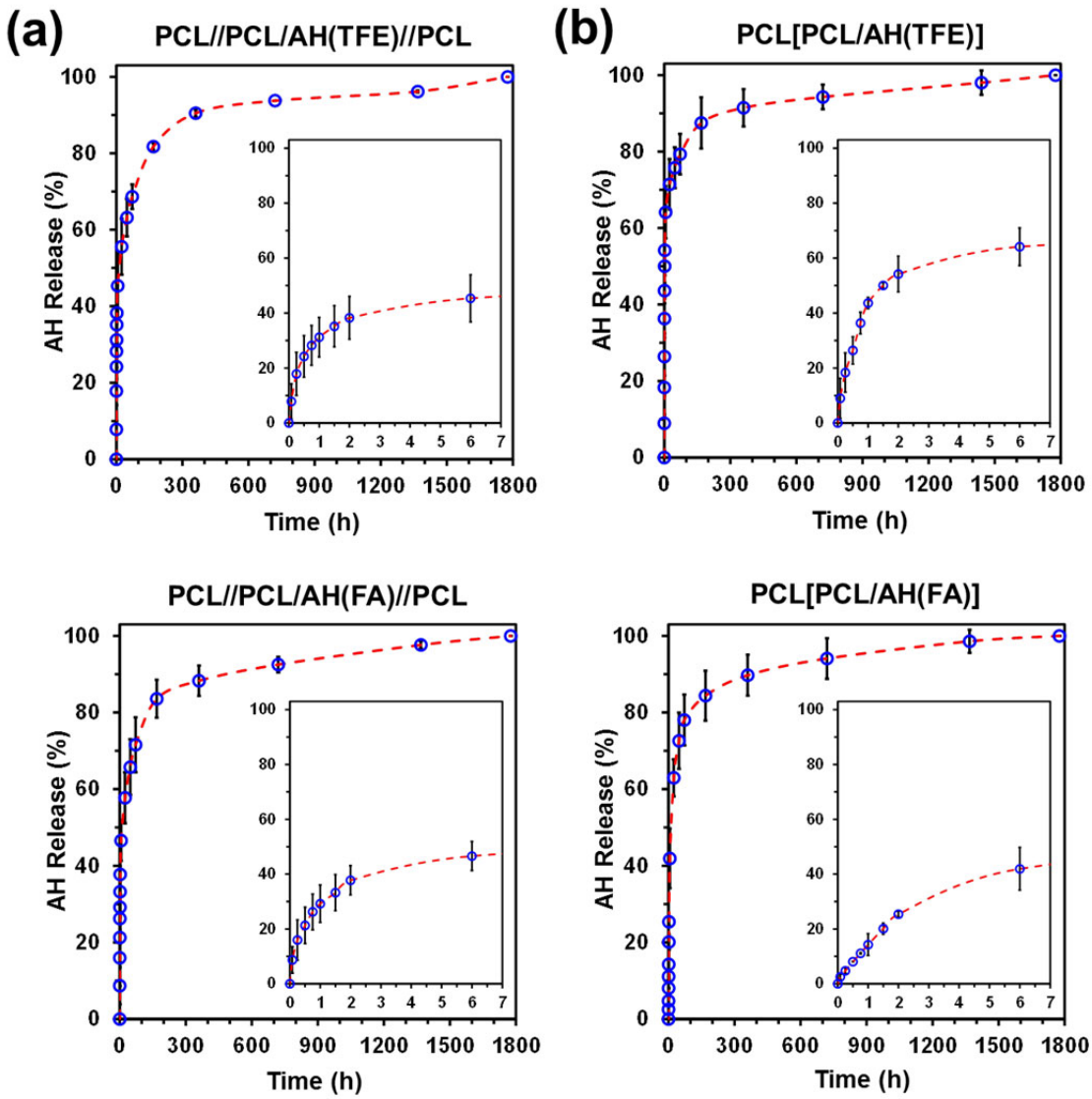
(a)
PCL//PCL/AH(TFE)//PCL
(b)
PCL[PCL/AH(TFE)]
PCL//PCL/AH(FA)//PCL
PCL[PCL/AH(FA)]
AH Release (%)
Time (h)

Figure 7

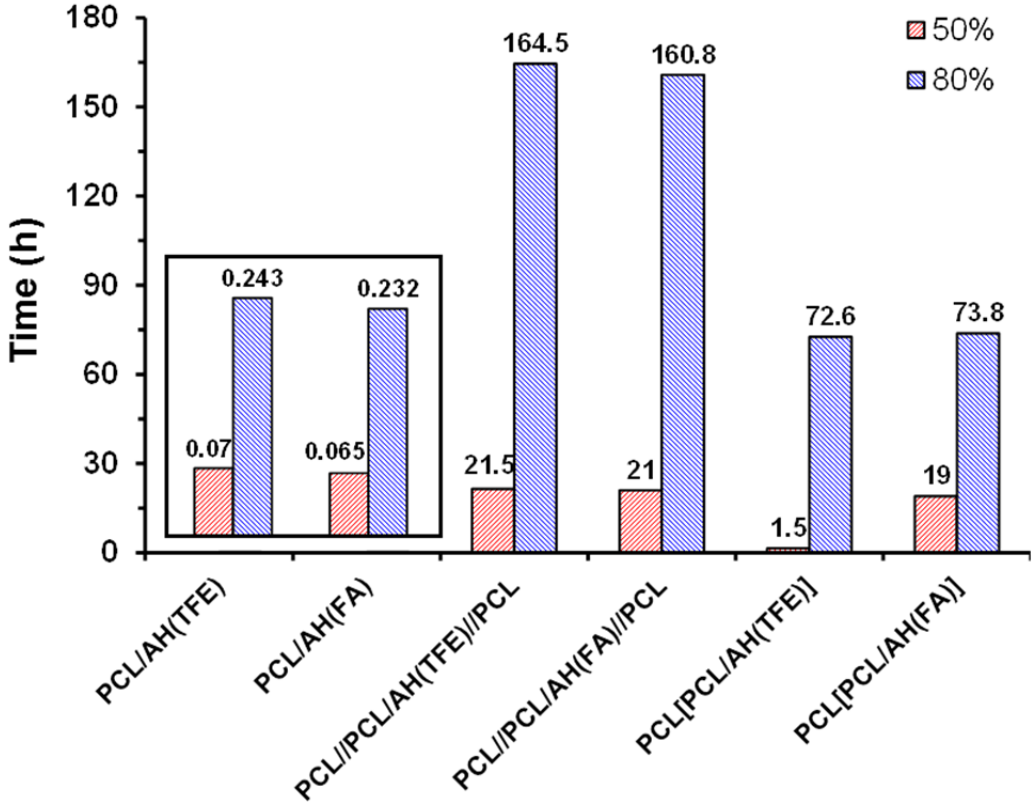
Time (h)
180
150
120
90
60
30
0
50%
80%
0.07
0.243
0.065
0.232
21.5
164.5
21
160.8
1.5
72.6
19
73.8
PCL/AH(TFE)
PCL/AH(FA)
PCL//PCL/AH(TFE)//PCL
PCL//PCL/AH(FA)//PCL
PCL[PCL/AH(TFE)]
PCL[PCL/AH(FA)]

Figure 8

Table of Contents

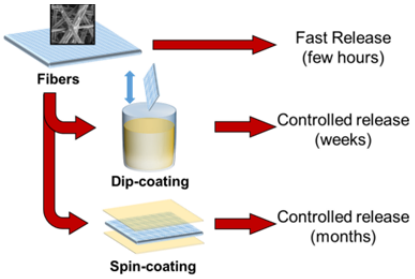

TOC text: The release of bioactive ambroxol, a pharmacological chaperone for Gaucher disease, from polyester scaffolds has been regulated (from a few hours to months) by controlling their geometry. For this purpose, the utilization of electrospun fibers (release rate: few hours) has been combined with dip-coating and spin coating techniques (release rate: weeks and months, respectively).

TOC keyword: Release regulation